9-27-2018

Finite-time Sliding Mode and Super-twisting Control of Fighter Aircraft

Kaushik Raj
University of Nevada, Las Vegas, raj@unlv.nevada.edu

Venkatesan Muthukumar
University of Nevada, Las Vegas, venkatesan.muthukumar@unlv.edu

Sahjendra N. Singh
University of Nevada, Las Vegas, sahjendra.singh@unlv.edu

Keum W. Lee
Catholic Kwandong University

Finite-Time Sliding Mode and Super-Twisting Control of Fighter Aircraft

Kaushik Raj[a,*], Venkatesan Muthukumar[a,**], Sahjendra N. Singh[a], Keum W. Lee[b]

[a] *Department of Electrical and Computer Engineering*
University of Nevada Las Vegas, Las Vegas, NV 89154-4026
[b] *Department of Electronic Engineering*
Catholic Kwandong University, Gangwon 25601, Republic of Korea

Abstract

The development of two nonlinear robust higher-order flight control systems for roll-coupled maneuvers of fighter aircraft with uncertain parameters is discussed in this article. The objective is to independently control the output variables (roll angle, pitch angle and sideslip angle), using aileron, elevator and rudder control surfaces. For a nominal model of aircraft, first, finite time stabilizing (FTS) control law based on the notion of geometric homogeneity is designed. Then, for robust control in the presence of parameter uncertainties, (i) a discontinuous sliding mode (DSM) control law and (ii) a super-twisting (STW) continuous control law are designed. It is shown that in the composite closed-loop system consisting of either (a) the FTS and DSM control laws or (b) the FTS and STW control systems, the output trajectory tracking error and its first-order derivative converge to the origin in finite time. Digital simulation results for a swept-wing fighter aircraft including the two composite control systems are obtained. These results show that each of the designed flight controllers accomplishes precise simultaneous large longitudinal and lateral maneuvers, despite uncertainties in the aerodynamic and inertia parameters, turbulence, and partial loss of control surface effectiveness.

Keywords: Aircraft flight Control, Robust finite time sliding mode control, Super-twisting control, Roll-coupled maneuver, longitudinal maneuvers, lateral maneuvers, nonlinear control systems, Wind Turbulence, Fault Tolerance,

*Principal corresponding author
**Corresponding author
Email addresses: raj@unlv.nevada.edu (Kaushik Raj), vm@unlv.nevada.edu (Venkatesan Muthukumar)

1. Nomenclature

I_x, I_y, I_z	=	Roll, Pitch, Yaw Moments of inertia about principal axes ($kg - m^2$)
$i_1 = (I_z - I_y)/I_x$		
$i_2 = (I_z - I_x)/I_y$	=	Non dimensional inertia coefficients
$i_3 = (I_y - I_x)/I_x$		
V	=	Velocity of the aircraft center of mass (km/sec)
g	=	Gravitational acceleration (m/sec^2)
α, β	=	Angle of attack ($radian$), sideslip angle ($radian$)
θ, ϕ	=	Pitch angle ($radian$), Roll angle ($radian$)
$\delta a, \delta r, \delta e$	=	Aileron, rudder and elevator deflection angles ($radian$)
l	=	Rolling moment per $I_x(1/sec^2)$
m	=	Pitching moment per $I_y(1/sec^2)$
n	=	Yawing moment per $I_z(1/sec^2)$
y	=	Side force (over aircraft mass and speed) $(1/sec)$
p, q, r	=	Components of angular velocity ($radian/sec$)
u, v, w	=	Components of velocity(m/sec)
X, Y, Z	=	Components of Force(m/sec)
x_1, x_2, x_3	=	State variables
u_c, v_f, v_d	=	Control signals

2. Introduction

Advanced fighter aircraft are expected to be highly maneuverable. Traditionally, aircraft flight controllers are designed by linearizing non-linear aircraft models at a large number of operating points [1–3] and then gain scheduling is used to cover the entire flight envelope [3]. But the gain scheduling is a comparatively difficult task to achieve in a large flight envelope. Various design methods, such as optimal control, H_∞ robust control, pole placement, etc. [4–6], have been used for flight control of linear aircraft models in the past. However, the equations of motion of aircraft include nonlinear aerodynamic forces and moments. At the high angle of attack, the aerodynamic forces and moments exerted on the aircraft depend on the past history of the flow. When aircraft perform high roll rate maneuvers, mainly two precarious situations are encountered: the first one is an instability of the short-period longitudinal and directional oscillations; and the second is auto-rotational rolling, in which the fighter can suddenly jump to a higher roll-rate, where, additionally, controls can become inefficient. All these phenomena can lead to a very high angle of attack or sideslip angle, causing unusual loading on the structure, leading to accidents [7–9]. Limitations of linear controllers can be overcome by performing input-output linearization (also termed as nonlinear dynamic inversion (NDI)) [10–18]. This method is used for decoupling the dynamics of selected controlled output variables by canceling the nonlinear functions present in the model; then linear stable tracking error dynamics are obtained through feedback of additional signals. Evidently, for exact cancellation, the dynamics of an aircraft must be known precisely. Variable structure controllers (VSC) have been designed [19–24] for nonlinear aircraft models in the presence of uncertainties. However, VSC controllers are discontinuous functions of state variables. Even

though some smoothing of control law can be done in the boundary layer, that might cause a terminal tracking error. Nonlinear adaptive flight controllers based on a back-stepping control method [25–32] have been designed for large parametric uncertainties and unknown functions in the model. The back-stepping design method is completed in several steps because this method is iterative in nature. The number of steps required depends on the relative degree of the controlled output variables. Also, neural networks(NN) based flight control systems have been designed [32–35]. Researchers in references [28, 30], have designed an adaptive flight controller with state and control constraints. These adaptive flight controllers belong to the class of certainty-equivalence adaptive control systems. In these cited controllers, the parameter estimates obtained by integral update laws are directly used. References in [36–38], propose non-certainty-equivalence adaptive control systems based on immersion and invariance (I&I) methods for control of an aircraft. Adaptive control of this model using ten independently actuated control surfaces with a bound on the uncertainty input matrix is given in the paper [39]. From the viewpoint of implementation, adaptive control laws are not simple because the parameter estimator needs to estimate a large number of aerodynamic parameters.

Also, considerable effort has been made in the past to analyze stability properties of fighter aircraft. The analysis shows that aircraft exhibit rich dynamical behavior in rotationally-coupled maneuvers. Based on the bifurcation methods and pseudo-steady-state analysis, authors have observed that roll-coupling can lead to an undesirable jump phenomenon and a rapid divergence of sideslip angle in the transient phase for certain combinations of control surface deflections. Bifurcation theory, invented by Poincare to analyze nonlinear systems, was first applied to the cross-coupling problems mentioned in [7], and then extended to the fully nonlinear problem of flight at a high angle of attack (α) [9, 40–42]. Researchers have developed the finite time stabilizing controllers for the fighter aircraft [43]. These class of controllers exhibits stronger robustness properties, compared to asymptotically stabilizing control systems.

The adaptive flight controllers can achieve only asymptotic stability. Some research related to finite time flight control systems has also been produced in references [20–23, 25, 44–49]. Finite-time control law for a hypersonic aircraft and a super-twisting guidance law have been designed in the reference [50]. However, it seems that a study related to finite time control laws for roll-coupled maneuvers of fighter aircraft remains due. Therefore, it is imperative to explore the applicability of finite time control methodologies for simultaneous longitudinal and lateral maneuvers, and for avoiding roll-coupled instabilities of fighter aircraft in the presence of uncertainties.

This article develops two robust finite time control systems for the roll-coupled maneuvers of fighter aircraft with uncertain inertia and aerodynamic parameters. The objective is to control output variables: roll angle, pitch angle, and sideslip angle using the aileron, elevator, and rudder deflection angles. A robust higher order sliding mode controller has been designed for this aircraft model [43]. But this controller needs to obtain the estimates of the derivatives of the angle of attack, and sideslip angle using a high gain observer (HGO). The introduction of an HGO increases the complexity of controllers from the implementation point of view, and moreover, a high gain feedback is not desirable in the presence of sensor noise. The two composite controllers (FTS with DSM and FTS with STW laws) designed here are sufficiently robust, and therefore, obviate the need for estimation of the derivatives of output variables.

The motivation to design such controllers stems from the fact that closed-loop finite time control systems have

stronger stability properties in comparison to asymptomatically stable feedback systems. Also, the finite time sliding mode controllers and super twisting controllers have not been applied for this swept-wing fighter aircraft model.

The contributions of this article are five-fold: First, a finite time stabilizing (FTS) nonlinear flight control law for a nominal aircraft model with assumed parameters, based on the notion of geometric homogeneity, is designed. Second, a discontinuous sliding mode (DSM) flight controller is developed to counter the effect of uncertainties in the model. In the closed-loop system, including the nominal finite time stabilizing (FTS) control law and the discontinuous sliding mode (DSM) control signal, finite time control of the roll angle (ϕ), pitch angle (θ), and sideslip angle (β) is accomplished. Discontinuous sliding mode control law might cause a control chattering phenomenon. Third, for robust control, a super-twisting (STW) sliding mode control law is designed. The STW control law is a continuous function of the state variables. In the closed-loop system, using the FTS and STW control laws, a finite time control of the aircraft is accomplished. Furthermore, this composite control system has the ability to attenuate undesirable control chattering. It is shown that in a closed-loop system, including the composite control law ((i) FTS with DSM, or (ii) FTS with STW control signals), the trajectory tracking error and its first derivative converge to zero in finite time. Fourth, using similar steps, composite control systems (FTS with DSM and FTS with STW laws) for finite time control of the roll angle (ϕ), angle of attack (α), and sideslip angle (β) are designed, but the details of derivation are not shown here in order to save space. Fifth, simulation results for a nonlinear swept-wing fighter aircraft are obtained, which show that the designed composite controllers accomplish satisfactory simultaneous longitudinal and lateral maneuvers of (ϕ, θ, β) or (ϕ, α, β), despite parametric uncertainties. It is pointed out that the structure of the derived flight controllers is simple compared to adaptive control laws in which a large number of aerodynamic parameters must be estimated.

The rest of the article is organized as follows: In section 3, the model of the fighter aircraft is described and control objectives are formulated. Section 4 presents the FTS, DSM, and STW controllers for the control of the output vector (ϕ, θ, β). This is followed by the introduction of the wind turbulence model in section 5. Simulation results are provided for the close-loop response of the aircraft, with and without wind gust under both composite controllers (FTS with DSM and FTS with STW laws), in Section 6. A comparison has been made between two controllers, and a table is provided to reflect the effect of varying speeds of a wind gust on response time and control input magnitude. Finally, the article concludes in section 7.

3. Aircraft Mathematical Model and Control Problem

In this work, the equations of motion of a swept-wing fighter aircraft derived by Hacker and Oprisiu [45], and Rhoads and Schuler [46] are considered. To study the rolling pull-out maneuver, an F-80 aircraft is instrumented under various flight conditions to provide motion and load data. The model presented in the following Eq.(1) has the inertia coupling term pq in the yawing moment equation which is responsible for a large excursion. The model is developed by laying more emphasis on nonlinearities associated with a high roll rate to the dynamics of a large disturbance. Very few aerodynamic data for use in large-disturbance, relating to nonlinearities in terms of

sideslip and rolling velocity are available. The set of equations considered across the principal axes are given by the following equations (detailed notations and terminologies are provided in the references [45, 46]):

$$\begin{pmatrix} \dot{p} \\ \dot{q} \\ \dot{r} \\ \dot{\alpha} \\ \dot{\beta} \\ \dot{\phi} \\ \dot{\theta} \end{pmatrix} = \begin{pmatrix} l_\beta\ \beta + l_q\ q + l_r\ r + (l_{\beta\alpha}\ \beta + l_{r\alpha}\ r)\Delta\alpha + l_p\ p - i_1\ q\ r \\ \bar{m}_\alpha\ \Delta\alpha + \bar{m}_q\ q + i_2\ p\ r - m_{\dot{\alpha}}\ p\ \beta + m_{\dot{\alpha}}\ (g_0/V)\ (cos\theta\ cos\phi - cos\theta_0) \\ n_\beta\ \beta + n_r\ r + n_p\ p + n_{p\alpha}\ p\ \Delta\alpha - i_3\ p\ q + n_q\ q \\ q - p\ \beta + z_\alpha\ \Delta\alpha + (g_0/V)\ (cos\theta\ cos\phi - cos\theta_0) \\ y_\beta\ \beta + p\ (sin\alpha_0 + \Delta\alpha) - r\ cos\alpha_0 + (g_0/V)\ cos\theta\ sin\phi \\ p + q\ tan\theta\ sin\phi + r\ tan\theta\ cos\phi \\ q\ cos\phi - r\ sin\phi \end{pmatrix}$$

$$+ \begin{pmatrix} \tilde{l}_{\delta a} & l_{\delta r} & 0 \\ 0 & 0 & \bar{m}_{\delta e} \\ \tilde{n}_{\delta a} & n_{\delta r} & 0 \\ 0 & 0 & z_{\delta e} \\ y_{\delta a} & y_{\delta r} & 0 \\ 0 & 0 & 0 \\ 0 & 0 & 0 \end{pmatrix} \begin{pmatrix} \delta a \\ \delta r \\ \delta e \end{pmatrix} \tag{1}$$

where $\tilde{l}_{\delta a} = l_{\delta a} + l_{\alpha\delta a}\ \Delta\alpha$, $\tilde{n}_{\delta a} = n_{\delta a} + n_{\alpha\delta a}\ \Delta\alpha$, $\overline{m}_{\delta e} = m_{\delta e} + m_{\dot{\alpha}}\ z_{\delta e}$, $\Delta\alpha = \alpha - \alpha_0$,
and α_0 is the equilibrium value. Here, p, q, and r denote the angular velocity component in the aircraft fixed frame, ϕ is the roll angle, and θ is the pitch angle. This mathematical model of the aircraft ignores speed variations and contains only a simple representation of the aerodynamic nonlinearities. Assuming that $u \cong V$ and the velocity components v and w are small, one has the sideslip angle $\beta \cong v/V$ and the angle of attack $\alpha \cong w/V$. The subscripts α, β, θ, ϕ, $\dot{\alpha}$, p, q, r, δ_a, δ_r and δ_e denote the partial derivatives of the rolling, pitching and yawing moments (l, m and n) as well as of forces (y and z) with respect to respective quantity. For example $y_\beta = \frac{\partial y}{\partial \beta}$, $m_{\dot{\alpha}} = \frac{\partial m}{\partial \dot{\alpha}}$, $n_{\alpha\delta a} = \frac{\partial^2 n}{\partial \alpha\ \partial \delta a}$, etc. The authors point out that these assumptions are not essential for the derivation of the control law. In fact, one can include higher-order aerodynamic nonlinearities in the model and the speed variation could be controlled by a throttle control system.

First, it is interesting to examine the complexity in the dynamical behavior of the open-loop aircraft model. For this purpose, Eq.(1) with typical control surface deflection commands of $\delta_a = 25^o$, and $\delta_e = -5^o$ with $\delta_r = 0$ at the flight condition one (FC 1) is simulated. The parameters given in references [45, 46], for the two flight conditions, are listed in the appendix for convenience. Figure(1) shows the waveforms of p, α and β. It can be seen that the sideslip angle β undergoes a large excursion (almost 18 deg.) and the angular velocity p attains a very high value close to 690 deg/s) within 1.6 s. One observes that in the open-loop system, after the initial transient period, p, α, and β, exhibits persistent oscillations of growing amplitudes.

The Problem Statement:

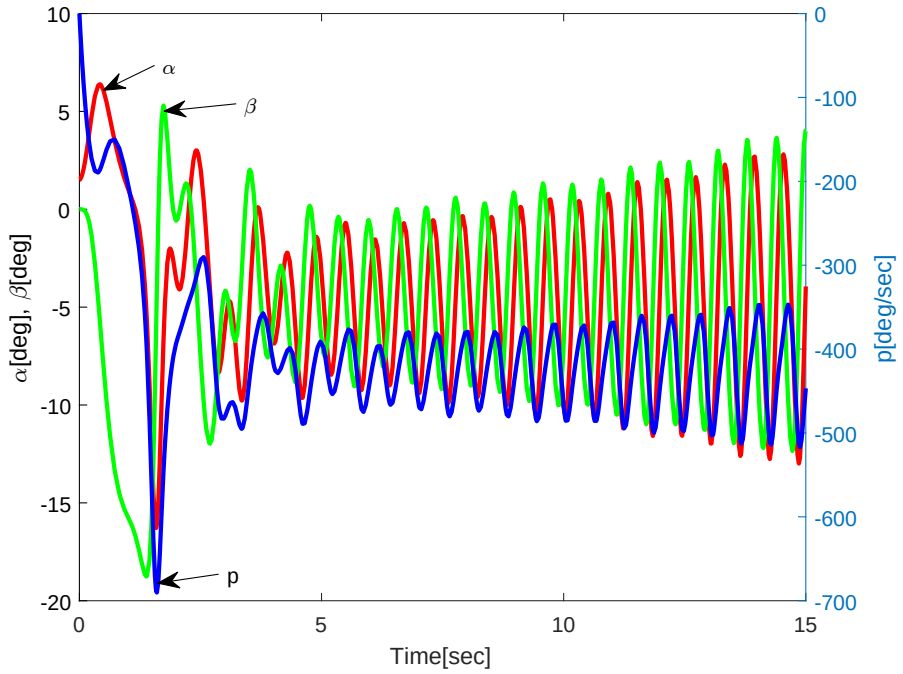

Figure 1: Aircraft response to combined aileron (25 deg) and elevator (-5 deg) inputs, showing the effect of coupling.

Define x_1=$(\phi,\ \theta,\ \beta)^T$, x_2= $(p,\ q,\ r)^T$, x_3= α and the state vector $x = (x_1^T,\ x_2^T,\ x_3)^T \in R^7$. The derivatives of $x_1,\ x_2$, and x_3 are obtained from Eq.(1).

$$\dot{x}_1 = \begin{bmatrix} 0 \\ 0 \\ y_\beta\ \beta + (g_0/V)\ \cos\theta\ \sin\phi \end{bmatrix}$$
$$+ \begin{bmatrix} 1 & \tan\theta\ \sin\phi & \tan\theta\ \cos\phi \\ 0 & cos\phi & -sin\phi \\ \sin\alpha_0 + \Delta\alpha & 0 & -\cos\alpha_0 \end{bmatrix} \begin{bmatrix} p \\ q \\ r \end{bmatrix} + \begin{bmatrix} 0 \\ 0 \\ y_{\delta a}\ \delta a + y_{\delta r}\ \delta r \end{bmatrix} \tag{2}$$
$$= f_1(\alpha,\ \beta,\ \phi,\ \theta) + G_1(\theta,\ \phi,\ \alpha,\ \beta)\ x_2 + g_\delta\ (\delta a,\ \delta r,\ \delta e)$$

where g_δ the control surface deflection-dependent vector function,

$$f_1 = \begin{bmatrix} 0 \\ 0 \\ y_\beta\ \beta + (g_0/V)\ \cos\theta\ \sin\phi \end{bmatrix}, G_1 = \begin{bmatrix} 1 & \tan\theta\ \sin\phi & \tan\theta\ \cos\phi \\ 0 & cos\phi & -sin\phi \\ \sin\alpha & 0 & -\cos\alpha_0 \end{bmatrix}$$

The derivative of x_2 is

$$\dot{x}_2 = \begin{bmatrix} \dot{p} \\ \dot{q} \\ \dot{r} \end{bmatrix} = \begin{pmatrix} l_\beta\ \beta + l_q\ q + l_r\ r + (l_{\beta\alpha}\ \beta + l_{r\alpha}\ r)\Delta\alpha + l_p\ p - i_1\ q\ r \\ \bar{m}_\alpha\ \Delta\alpha + \bar{m}_q\ q + i_2\ p\ r - m_{\dot{\alpha}}\ p\ \beta + m_{\dot{\alpha}}\ (g_0/V)\ (\cos\theta\ \cos\phi - \cos\theta_0) \\ n_\beta\ \beta + n_r\ r + n_p\ p + n_{p\alpha}\ p\ \Delta\alpha - i_3\ p\ q + n_q\ q \end{pmatrix}$$
$$+ \begin{pmatrix} \tilde{l}_{\delta a} & l_{\delta r} & 0 \\ 0 & 0 & \bar{m}_{\delta e} \\ \tilde{n}_{\delta a} & n_{\delta r} & 0 \end{pmatrix} \begin{pmatrix} \delta a \\ \delta r \\ \delta e \end{pmatrix}$$
$$= f_2(x) + G_2(\alpha)\ u_c \tag{3}$$

where $u_c = (\delta_a,\ \delta_r,\ \delta e)^T \in R^3$ is the control input vector,

$$f_2(x) = \begin{pmatrix} l_\beta\ \beta + l_q\ q + l_r\ r + (l_{\beta\alpha}\ \beta + l_{r\alpha}\ r)\Delta\alpha + l_p\ p - i_1\ q\ r \\ \bar{m}_\alpha\ \Delta\alpha + \bar{m}_q\ q + i_2\ p\ r - m_{\dot{\alpha}}\ p\ \beta + m_{\dot{\alpha}}\ (g_0/V)\ (\cos\theta\ \cos\phi - \cos\theta_0) \\ n_\beta\ \beta + n_r\ r + n_p\ p + n_{p\alpha}\ p\ \Delta\alpha - i_3\ p\ q + n_q\ q \end{pmatrix}$$

$$G_2(\alpha) = \begin{pmatrix} \tilde{l}_{\delta a} & l_{\delta r} & 0 \\ 0 & 0 & \bar{m}_{\delta e} \\ \tilde{n}_{\delta a} & n_{\delta r} & 0 \end{pmatrix}$$

$$\dot{x}_3 = \dot{\alpha} = q - p\ \beta + z_\alpha\ \Delta\alpha + (g_0/V)\ (cos\theta\ cos\phi - cos\theta_0) \tag{4}$$

It is assumed that the model parameters are not precisely known. The objective is to design robust flight control systems for the control of output vector $y_1 = x_1 = (\phi,\ \theta,\ \beta)^T$. Suppose that $\phi_r(t),\ \theta_r(t),$ and $\beta_r(t)$ are given smooth reference trajectories. Where, $y_{1r} = x_{1r} = (\phi_r(t),\ \theta_r(t),\ \beta_r(t))^T$. The authors are interested in designing robust control systems, such that in a closed-loop system, the trajectory error $(y_{1r} - y_1)$ converges to zero in finite

time, despite uncertainties in the system. It is noted that by proper selection of reference trajectories, desirable roll-coupled maneuvers can be completed.

4. Higher-Order Sliding Mode and STW (ϕ, θ, β) Control Laws

In this section, the derivation of a higher-order sliding mode flight controller for the finite time control of the selected output vector $y_1 = (\phi,\ \theta,\ \beta)^T$ is considered. The first composite control system consists of: a finite time stabilizing (FTS) control law based on the notion of geometric homogeneity (Bhat and Berstein [20]) for a nominal model of the aircraft, and a discontinuous sliding mode (DSM) control law (Defoort et al. [21]) to nullify the effect of uncertainties. However, the discontinuity in the DSM law can cause undesirable control chattering phenomenon. To obtain smoother responses in the presence of uncertainties, a second composite control system, consisting of the FTS control law and a super-twisting control law is developed. Unlike the first composite control system, the second controller is a continuous function of the state variable.

Define the tracking error associated with y_1 as :

$$\tilde{x}_1 = x_1 - x_{1r} = (\phi - \phi_r,\ \theta - \theta_r,\ \beta - \beta_r)^T.$$

For the purpose of design, a simplified model obtained through ignoring the input-dependent function $g_\delta(u_c)$ in Eq.(2), is considered. This is justified because control surfaces are principally moment producing devices, and therefore their contributions in the $\dot{\alpha}$ and $\dot{\beta}$ are small. For the simplified model, differentiating $\tilde{x}_1$ twice gives

$$\ddot{\tilde{x}}_1 = \begin{bmatrix} 0 \\ 0 \\ y_\beta\ \dot{\beta} + (g_0/V)\ (-\sin\theta\ \ \sin\phi\ \dot{\theta} + \cos\theta\ \ \cos\phi\ \dot{\phi}) \end{bmatrix} + \dot{G}_1\ x_2 + G_1\ (f_2(x) + G_2\ u_c) - \ddot{x}_{1r}$$

$$= df_1(x) + \dot{G}_1\ x_2 + G_1(f_2 + G_2\ u_c) - \ddot{x}_{1r} \triangleq f_3(x) + B(x)\ u_c \tag{5}$$

where, $df_1 \in R^3$ denotes the vector function in the square bracket,

$$f_3 = df_1(x) + \dot{G}_1\ x_2 + G_1\ f_2 - \ddot{x}_{1r},\ \text{and}\ B(x) = G_1(x)\ G_2(\alpha)$$

where, f_3 and B are a 3×3 matrix.

The aircraft parameters are assumed to be not known. For the derivation of the control law, the uncertain vector function $f_3(x)$ and the matrix $B(x)$ are decomposed as $f_3(x) = f_3^*(x) + \Delta f_3(x,\ t)$ and $B(x) = B^*(x) + \Delta B(x)$, respectively, where $f_3^*(x)$ and $B^*(x)$ are the nominal values, and Δf_3, and ΔB are uncertain parts of f_3 and B. It is assumed that the matrix $B(x)$ and $B^*(x)$ are nonsingular in the admissible region of interest in the state space. Then $\ddot{\tilde{x}}_1$ takes the form

$$\ddot{\tilde{x}}_1 = (f_3^*(x) + \Delta f_3(x)) + (B^*(x) + \Delta B(x))\ u_c \tag{6}$$

In view of Eq.(6), a control signal is chosen of the form

$$u_c = (B^*(x))^{-1}[-f_3^*(x) + v_f + v_d] \tag{7}$$

where $v_f \in R^3$ and $v_d \in R^3$ are new control signals yet to be determined.

Define $\xi_1 = \tilde{x}_1 = [\xi_{11},\ \xi_{12},\ \xi_{13}]^T \in R^3$, $\xi_2 = \dot{\tilde{x}}_1 = [\xi_{21},\ \xi_{22},\ \xi_{23}]^T \in R^3$, and $\xi = [{\xi_1}^T, {\xi_2}^T]^T \in R^6$. Then, using Eqs. (6) and (7), the tracking error dynamics can be written as

$$\dot{\xi} = \begin{bmatrix} \xi_2 \\ \Delta f_3(x,t) - \Delta B(x)(B^*(x))^{-1} f_3^*(x) + (I_{3\times 3} + \Delta B(x)(B^*(x))^{-1})(v_f + v_d) \end{bmatrix} \tag{8}$$

The authors are interested in designing a second-order sliding mode flight controller for the trajectory control of ξ.

Definition 1: For the system Eq.(8) describing the ξ dynamics, define a manifold as $\mathscr{M}_2 = \{\xi \in R^6 :\ \xi_1 = 0,\ \dot{\xi}_1 = \xi_2 = 0\}$. The manifold $\mathscr{M}_2$ is a second-order sliding set, and the motion of the system confined on $\mathscr{M}_2$ is termed as the second-order sliding mode.

The second-order sliding motion for the system (8) will be accomplished by the choice of the control signals v_f and v_d. Assuming that v_d is zero, the control input v_f is designed to achieve a finite time trajectory control of ξ_1 of the system (8) without uncertainties (i. e., $\Delta f_3 = 0$, $\Delta B = 0$). Then, a switching control vector v_d is designed to nullify the effect of uncertain functions. Similar derivation using another set of output variable (ϕ, α, β) controllers can be designed. Results for output tracking are provided in the simulation section.

A. Finite Time Stabilizing (FTS) Flight Control Law v_f

The nominal ξ-dynamics with $v_d = 0$, obtained from Eq.(8) by setting $\Delta f_3 = 0$ and $\Delta B = 0$, can be written as

$$\dot{\xi}_1 = \xi_2;\ \dot{\xi}_2 = v_f \tag{9}$$

The system Eq. (9) is realized by a chain of two integrators. The objective is to select v_f to regulate $\xi \in R^6$ to zero in a finite time. Now, The definition of finite time stability is introduced in Bhat and Bernstein [20].

Definition 2: The equilibrium point $z = 0 \in R^n$ of a system $\dot{z} = h(z)$ is finite time stable if (i) it is stable (in the sense of Lyapunov), and (ii) there exists an open neighborhood $\mathscr{Z} \subset R^n$ of the origin and a function $T_s : \mathscr{Z} \to [0, \infty)$, called the settling time, such that for each $z_0 \in \mathscr{Z}$, the solution $z(t)$ remains in $\mathscr{Z}$ for all time $t \in [0,\ T_s(z_0))$, and $z(t)$ tends to zero, as t tends to $T_s(z_0)$.

The origin is said to be a globally finite-time-stable equilibrium if it is a finite time stable equilibrium with $\mathscr{Z} = R^n$. For finite-time stabilization of the system in Eq. (9), a judicious choice of control input v_f is made so that the closed-loop system becomes a homogeneous system ([20, 43]).

Definition 3: A vector field $h(z_1, ..., z_n) \in R^n$ is said to be homogeneous of degree $\mu \in R$ with dilation $(\nu_1, ..., \nu_n) \in ((0, \infty))^n$ if $h_i(p^{\nu_1} z_1, ..., p^{\nu_n} z_n) = p^{\mu+\nu_i}\ h_i(z)$, for $i = 1, ..., n$, $\forall z \neq 0$, and $\forall p > 0$, where $z = (z_1, ..., z_n)^T$ and h_i is the ith component of vector h.

Following Bhat and Bernstein [20], a finite time stabilizing control law $v_f = [v_{f1},\ v_{f2},\ v_{f3}]^T$ is selected of the form, $(i = 1,\ 2,\ 3)$,

$$v_{fi}(\xi_{1i},\ \xi_{2i},\ \xi_{3i}) = -k_{1i}\ sgn(\xi_{1i})\ |\xi_{1i}|^{\nu_{1i}} - k_{2i}\ sgn(\xi_{2i})\ |\xi_{2i}|^{\nu_{2i}} \tag{10}$$

The feedback gains k_{ji} are chosen such that the polynomial

$$\Pi(\lambda) = \lambda^2 + k_{2i}\lambda + k_{1i} \tag{11}$$

is Hurwitz. The exponents ν_{ji} are chosen to satisfy

$$\nu_{j-1,i} = \frac{\nu_{j,i}\ \nu_{j+1,i}}{2\nu_{j+1,i} - \nu_{j,i}},\ j = 2$$

$$\nu_{3i} = 1,\ \nu_{2i} = \nu_i \tag{12}$$

where $\nu_i \in (1 - \epsilon_{ni}, 1)$ and $\epsilon_{ni} \in (0, 1)$. In view of Eq.(10), one observes that the ith control signal v_{fi} is only the function of $\xi_{ji},\ j = 1, 2$; that is, ξ_{1i} and its first derivative. Thus, for example, the roll channel control signal is synthesized using the proportional and derivative terms of the roll trajectory error.

In the closed-loop system including the feedback signal v_f, one obtains decoupled homogeneous systems ($i = 1,\ 2,\ 3$)

$$\dot{\xi}_{ji} = \xi_{j+1,i},\ j = 1$$

$$\dot{\xi}_{2i} = -k_{1i}\ sgn(\xi_{1i})\ |\xi_{1i}|^{\nu_{1i}} - k_{2i}\ sgn(\xi_{2i})\ |\xi_{2i}|^{\nu_{2i}} \tag{13}$$

of negative degree $\mu_i = (\nu_i - 1)/\nu_i$, with dilation $(\nu_{1i}^{-1},\ \nu_{2i}^{-1})$, $(i = 1,\ 2)$. It is important to note that asymptotic stability of a continuous homogeneous system with a negative degree is equivalent to its global uniform finite time stability. According to a result of Bhat and Bernstein (2005) [20], there exists $\epsilon_{ni} \in (0,\ 1)$ such that, for every $\nu_i \in (1 - \epsilon_{ni},\ 1)$, the origin $\xi = 0$ of the subsystem Eq.(13) is finite time stable.

B. Discontinuous Sliding Mode (DSM) Control Law v_d

Now the design of the control signal v_d for nullifying the effect of uncertain functions is considered. The derivation of the control signal is based on the results of reference [47]. Therefore, the steps in design are briefly described for completeness.

For the design, similar to [47, 48], a sliding vector function $s(\xi_2,\ \xi_a) \in R^3$ of the form

$$s = \xi_2 - \xi_a \tag{14}$$

is considered, where $\xi_a \in R^3$ satisfies the differential Eq. given by

$$\dot{\xi}_a = v_f \tag{15}$$

The signal ξ_a is the integral of the nominal input v_f. Now the discontinuous signal v_d is designed to force the system trajectory to the sliding surface $s = 0$, despite uncertainties in the system. Differentiating s along the solution of Eq. (13) gives

$$\begin{aligned}\dot{s} &= [I_{3\times 3} + \Delta B(B^*)^{-1}]\ v_d + \Delta f_3(x) - \Delta B(x)(B^*(x))^{-1}(f_3^* - v_f) \\ &\doteq [I_{3\times 3} + \Delta B(B^*)^{-1}]\ v_d + \Delta d(x,\ t)\end{aligned} \tag{16}$$

where the uncertain vector function is

$$\Delta d(x, t) = \Delta f_3(x) - \Delta B(x)(B^*(x))^{-1}(f_3^* - v_f) \tag{17}$$

For the derivation of the control law v_d, consider a Lyapunov function

$$W(s) = (s^T s)/2 \tag{18}$$

Its derivative along the solution of Eq.(16) is

$$\dot{W} = s^T\ [(I_{3\times 3} + \Delta B(B^*)^{-1})\ v_d + \Delta d] \tag{19}$$

To this end, the following assumption on the uncertain functions is made:

Assumption 1: There exist a function $\eta_1(x,\ t)$ and a $\eta_0 \in [0,\ 1)$ such that the following inequalities hold:

$$||\Delta d(x,t)||_\infty = ||\Delta f_3(x) - \Delta B(x)(B^*(x))^{-1}(f_3^* - v_f)||_\infty \leq \eta_1(x,t) \tag{20}$$

$$||\Delta B(B^*)^{-1}||_\infty \leq \eta_0 < 1 \tag{21}$$

Then, using inequality Eq.(20) in (19) gives

$$\dot{W} \leq s^T(I_{2\times 2} + \Delta B(B^*)^{-1})\ v_d + ||s||_1.\ ||\Delta d||_\infty$$

$$\leq s^T(I_{3\times 3} + \Delta B(B^*)^{-1})\ v_d +\ \eta_1(x,t)\ ||s||_1 \tag{22}$$

where $||.||_1$ and $||.||_\infty$ denote 1 norm and ∞ norm. In view of Eq.(22), a discontinuous control law v_d is selected of the form

$$v_d = -G(x,t)\ sign(s) \tag{23}$$

where gain $G(x,t)$, is positive. Substituting (23) in (22) gives

$$\dot{W} \leq -G(x,t)\ ||s||_1 - G(x,t)\ s^T\ \Delta B(B^*)^{-1}\ sign(s) + \eta_1(x,t)\ ||s||_1 \tag{24}$$

Using the second inequality of Assumption 1, Eq.(24) gives

$$\dot{W} \leq -G(x,t)\ ||s||_1 + \eta_0\ G(x,t)\ ||s||_1\ ||sign(s)||_\infty + \eta_1(x,t)\ ||s||_1 \tag{25}$$

Because $||sign(s)||_\infty \leq 1$, one obtains

$$\dot{W} \leq -G(x,t)\ ||s||_1\ (1-\eta_0) + \eta_1(x,t)\ ||s||_1 \tag{26}$$

It follows that by selecting the switching gain according to

$$G(x,t) \geq (1-\eta_0)^{-1}\ [\eta_1 + \eta^*] \tag{27}$$

with $\eta^* > 0$ yields

$$\dot{W} \leq -\sqrt{2}\ \eta^*\ \sqrt{W} \tag{28}$$

This implies that s converges to zero in a finite-time and the trajectory remains confined to the sliding surface $s = 0$ for $t \geq T_r(s(0))$, where

$$T_r \leq W^{1/2}(s(0))(\sqrt{2}\ \eta^*)^{-1}$$

for all $s \in R^3$. It is interesting to note that during the sliding phase, the equivalent control signal v_{deqv} satisfies

$$\dot{s} = [I_{3\times 3} + \Delta B(B^*)^{-1}]\ v_{deqv} + \Delta d(x,t) = 0 \tag{29}$$

Thus one has

$$v_d = v_{deqv} = -[I_{3\times 3} + \Delta B(B^*)^{-1}]^{-1}\Delta d(x,t) \tag{30}$$

Now in view of the definition of Δd in Eq.(17), substituting (30) in (8) gives the homogeneous system

$$\dot{\xi} = [\xi_2^T,\ v_f^T]^T \tag{31}$$

It has already been shown that this system, with v_f given in Eq.(10), is finite time stable. Thus, one concludes that the trajectory $\xi(t)$ of the system Eq.(8) converges to $\xi = 0$ in finite time. This implies that the tracking error $(\tilde{\phi},\ \tilde{\theta},\ \tilde{\beta})$ converges to zero as well in finite time. This completes the design of the composite control system consisting of the FTS and DSM laws for finite time control of the output vector y_1.

C. Finite Time Super-Twisting (STW) Flight Control Law The DSM control law v_d in Eq.(23) is a discontinuous function of the state variables. It is well known that in the closed-loop system, discontinuous signals can cause a control chattering phenomenon. In this subsection, an STW control law v_d of the form [47, 48] is designed instead, which is continuous, and therefore, attenuates the adverse effect of actuator chattering.

The derivation of the STW law begins with Eq. (16) which can be written as

$$\dot{s} = v_d + d_a \tag{32}$$

where the uncertain vector function is

$$d_a = \Delta B(B^*)^{-1}\ v_d + \Delta d(x,\ t) \tag{33}$$

The objective is to design a continuous signal v_d, such that s and its derivative $\dot{s}$ converge to zero in finite time. The derivation is based on the design technique provided in reference [47, 48].

The STW control signal v_d is selected as

$$v_d = -p_0\ |s|^{1/2}\ sign(s) + \eta \tag{34}$$

$$\dot{\eta} = -p_1\ sign(s)$$

where p_0 and p_1 are appropriate positive constants. Substituting Eq.(34) in Eq.(32) gives

$$\dot{s} = d_a - p_0\ |s|^{1/2}\ sign(s) + \eta \tag{35}$$

$$\dot{\eta} = -p_1\ sign(s)$$

Define $\eta_a = d_a + \eta$ then Eq.(35) gives

$$\dot{s} = -p_0\ |s|^{1/2}\ sign(s) + \eta_a$$

$$\dot{\eta_a} = -p_1\ sign(s) + \Gamma_u(t) \tag{36}$$

where $\Gamma_u = d(d_a)/dt = (\Gamma_{u1},\ \Gamma_{u2},\ \Gamma_{u3})^T$.

It is assumed that the trajectories of the aircraft system evolve in a region Ω, in which the uncertain function Γ_u satisfies for $(i = 1,\ 2,\ 3)$

$$|\Gamma_{ui}| \leq L_{pi} \tag{37}$$

where L_{pi} is a positive constant. Let s_i and η_{ai} be the ith elements of s and η_a. For stability analysis, a new coordinate vector $\zeta_i \in R^2$ is defined for $(i = 1, 2, 3)$ as

$$\zeta_i = [\zeta_{i1},\ \zeta_{i2}]^T = [|s_i|^{1/2}\ sign(s_i),\ \eta_{ai}]^T$$

Now it is easy to verify that

$$\dot{\zeta}_i = \frac{1}{|s_i|^{1/2}} \begin{bmatrix} -0.5\ p_0 & 0.5 \\ -p_1 & 0 \end{bmatrix} \zeta_i + \frac{1}{|s_i|^{1/2}} \begin{bmatrix} 0 \\ \Gamma_{ui}\ sign(s_i)\ \zeta_{i1} \end{bmatrix} \tag{38}$$

$$= \frac{1}{|s_i|^{1/2}} [F\ \zeta_i + (0,\ v_{\Gamma i})\ \zeta_{i1}^T]$$

where $v_{\Gamma i}$=Γ_{ui} sign(s_i), and F is given in Eq.(38). The matrix F is Hurwitz.

Moreno, in [51, 52], established stability of $\zeta_i = 0$ by using the Lyapunov method. Other methods for stability analysis, such as the geometrical method [48] and stability by homogeneity properties [47], can be used as well. Consider a Lyapunov function

$$W_i(\zeta_i) = \frac{1}{2} {\zeta_i}^T \begin{bmatrix} 4p_1 + {p_0}^2 & -p_0 \\ -p_0 & 2 \end{bmatrix} \zeta_i \doteq {\zeta_i}^T P\ \zeta_i \tag{39}$$

where P defined in Eq.(39) is a positive definite symmetric matrix ($P > 0$). The derivative of W_i is

$$\dot{W}_i = -\frac{p_0\ {\zeta_i}^T}{2|s_i|^{1/2}} \begin{bmatrix} 2p_1 + {p_0}^2 + 2v_{\Gamma i} & -p_0 - 2{p_0}^{-1}\ v_{\Gamma i} \\ -p_0 - 2{p_0}^{-1}\ v_{\Gamma i} & 1 \end{bmatrix} \zeta_i \tag{40}$$

Because $|v_{\Gamma i}| \leq L_{pi}$, this implies that $\dot{W}_i$ satisfies

$$\dot{W}_i \leq -\frac{p_0\ {\zeta_i}^T}{2|s_i|^{1/2}} \begin{bmatrix} 2p_1 + {p_0}^2 - 2L_p & -p_0 - 2{p_0}^{-1} L_{pi} \\ -p_0 - 2{p_0}^{-1} L_{pi} & 1 \end{bmatrix} \zeta_i \doteq -\frac{1}{|s_i|^{1/2}} {\zeta_i}^T Q_i\ \zeta_i \tag{41}$$

where, Q_i is a symmetric matrix. Q_i is positive definite if, and only if, $2p_1 + {p_0}^2 - 2L_{pi}$ and determinant of $Q_i > 0$. For a given L_{pi}, there always exits p_0 and p_1 such that $Q_i > 0$. Let $\lambda_m(.)$ and $\lambda_M(.)$ denote minimum and maximum eigenvalues of a matrix. Now,

$$\lambda_m(P)||\zeta_i)||^2\ \leq W_i \leq \lambda_M(P)||\zeta_i||^2;\ \lambda_m(Q_i)\ ||\zeta_i||^2 \leq {\zeta_i}^T Q_i\ \zeta_i$$

$$|s_i|^{1/2} \leq ||\zeta_i|| \leq \sqrt{W_i/\lambda_m(P)}$$

From Eq.(41) one can show that the derivative of W_i satisfies

$$\dot{W}_i \leq -\gamma\ {W_i}^{1/2};\ \gamma = \lambda_m(Q_i)\ \lambda_M^{-1}(P)\sqrt{\lambda_m(P)} \tag{42}$$

Now, by integrating Eq.(42), one can show that $\zeta_i = (|s_i|^{1/2}\ sign(s_i),\ \eta_{ai})^T$ converges to zero in finite time. Of course, this stability analysis can be done for finite time control of state subvectors $\zeta_j = (|s_j|^{1/2}\ sign(s_j),\ \eta_{aj})^T$, $j = 1,\ 2,\ 3$. Thus setting $(s,\ \eta_a) = 0$ in Eq. (36) gives $\dot{s} = 0$ in finite time. Setting $\dot{s} = 0$ in Eq.(32) gives $v_d = -d_a$, which implies that v_d cancels all the uncertain functions in Eq. (8) and Eq. (8) becomes

$$\dot{\xi}_1 = \xi_2;\ \dot{\xi}_2 = v_f \tag{43}$$

In view of v_f given in Eq.(10), it follows that in a closed-loop system, including the composite controller consisting of the FTS and STW control laws, the output tracking error $\xi_1 = (\tilde{\phi},\ \tilde{\theta},\ \tilde{\beta})^T$ and its derivative converge to zero in finite time. This completes the design of the composite control system (FTS and STW laws).

Remark 1: In the literature, design of control laws for the regulation of the output vector $(\phi,\ \alpha,\ \beta)$ has also been considered using various control techniques. The authors have also designed the FTS, DSM, and STW control laws for the finite time control of $(\phi,\ \alpha,\ \beta)$. However, here only simulation results will be presented and the derivation of control signals will not be given for the sake of space [14, 25, 43].

Stability of Internal Dynamics

It is of interest to examine the stability properties of the internal dynamics of aircraft because each of the selected outputs has a relative degree of two, but the model has seven state variables. Thus there exists an internal dynamics(zero dynamics) of dimension one. Consider the closed-loop system including the control law for finite time control of $y_1 = (\phi,\ \theta,\ \beta)^T$. Noting that $(p,\ q,\ r)$ can be expressed as a function of y_1, and $\dot{y}_1$, the remaining variable α represents the state of internal (residual) dynamics. Assuming that y_1 is controlled to the terminal value $(\phi = 0,\ \theta = \theta_0,\ \beta = 0)^T$, it is easily shown that the internal dynamics take the form

$$\dot{\alpha} = z_\alpha\ \Delta\alpha$$

Because z_α is negative, the equilibrium point is exponentially stable.

Now let us obtain the internal dynamics if the chosen output vector as $y_2 = (\phi,\ \alpha,\ \beta)^T$. For this case, the residual dynamics are described by the pitch angle θ. Assuming that in a closed-loop system, one has $y_2 = (0,\ \alpha_0,\ 0)^T$ and its derivative is identically zero. Then one can show that the internal dynamics take the form

$$\dot{\theta} = -(g_0/V)(\cos\theta - \cos\theta_0)$$

which can be linearized to obtain

$$\dot{\tilde{\theta}} = (g_0/V)\ sin\theta_0\ \tilde{\theta}$$

where $\tilde{\theta} = \theta - \theta_0$. This shows that internal dynamics are stable if θ_0 is negative, and is unstable if θ_0 is positive. However, one should note that as long as θ remains within $\pi/2$, the control law is well defined. (Note that the model has a singularity at $\theta = \pm\pi/2$.) Moreover, the authors have not considered the design of the outer loop. In the complete closed-loop system including the inner and outer control loops, even the controller designed for α control accomplishes intended maneuvers [14, 25]. Of course, for high performance, it is useful to use different autopilots in different phases of flight.

5. Wind Turbulence model

Various wind turbulence models have been used in the literature [53, 54]. Turbulence is a stochastic process represented by velocity spectra. It is assumed that in a turbulence field, time variations are statistically equivalent to distance variations in traversing the field. It is assumed that turbulence effects produce changes in aerodynamic forces and moments only. For altitude hold, the vertical component of the gust(w_g) [53, 54] is critical. In this case, the angle of attack (α_A) to be used in an aircraft equation of motion is:

$$\alpha_A = \alpha - \frac{w_g}{V} \tag{44}$$

The most common wind turbulence models are generated by either *Von Kármán* or Dryden spectral representations, by filtering the band limited white noise with an appropriate forming filter which is derived from the spectral representation. This article uses a continuous *Von Kármán* filter. A unit variance band-limited white noise signal is then passed through the *Von Kármán* forming filter. *Von Kármán* spectra are curve fitted to a satisfactory approximation because it is not factorable. The *Von Kármán* spectra is

$$\Phi_{w_g}(w) = \sigma_w^2 \frac{L_w}{\pi} \frac{1 + \frac{8}{3}(1.339 L_w \ \frac{w}{V})^2}{[1 + (1.339 L_w)^2]^{11/6}} \tag{45}$$

Spectral density is a second order moment and the continuous filter obtained from it is a transfer function

$$H_{w_g}(\hat{s}) = \frac{\sigma_w \sqrt{\frac{L_w}{V}}(1 + 2.7478 \frac{L_w}{V} \ \hat{s} + 0.3398(\frac{L_w}{V})^2 \ \hat{s}^2)}{1 + 2.9958 \frac{L_w}{V} \ \hat{s} + 1.9754(\frac{L_w}{V})^2 \ \hat{s}^2 + 0.1539(\frac{L_w}{V})^3 \ \hat{s}^3} \tag{46}$$

where, L_w= scale of vertical turbulence, σ_w= vertical gust intensity, and w is frequency. (Note that $\hat{s}$ in the transfer function H denotes the Laplace variable Open-loop response of the aircraft under turbulence is shown in figure (2).

Fault-Tolerance

Performance and stability of the aircraft can be compromised due to the occurrences of different types of faults. Partial damage of control surfaces (elevator, aileron, and rudder) can cause the variation of aircraft's stability and control derivatives which could diminish the control effectiveness. In this case, control derivatives (elements of input matrix B) change. For the derivation of control laws, it has been assumed that all the aerodynamic parameters are not precisely known. It is expected that DSM and STW flight control laws derived here can preserve the stability and yield the satisfactory performance after a brief transient following the instant of damage. In section 6, simulation results under turbulence and control surface degradation will be provided to demonstrate the robustness properties of the control laws.

At times aircraft can undergo severe faults such as freezing or lock-in-place and float situations. In these cases, a fault tolerant controller is required to preserve stability and recover performance of the aircraft system. A freezing or lock-type failure occurs when the control effectors get stuck in a particular position and do not respond to any commands. Whereas, in a float-type failure, control effectors float with its zero-moment position. For such kind of faults, control systems must have the ability to identify, detect and isolate the fault and reconfigure the structure of the control system using remaining healthy actuators to at least preserve the stability. Dedicated fault tolerant controllers capable of fault tolerating potential are designed to accommodate component failure automatically. Researches have devised various control schemes for fault tolerant controllers in the literature [55]. Moreover, to cover the entire gamut of the fault tolerant control problems, researchers may refer to these review papers [56, 57]. In recent survey papers, [58, 59] authors have provided several references for monitoring for fault diagnosis, damage detection which is relevant to any physical control system.

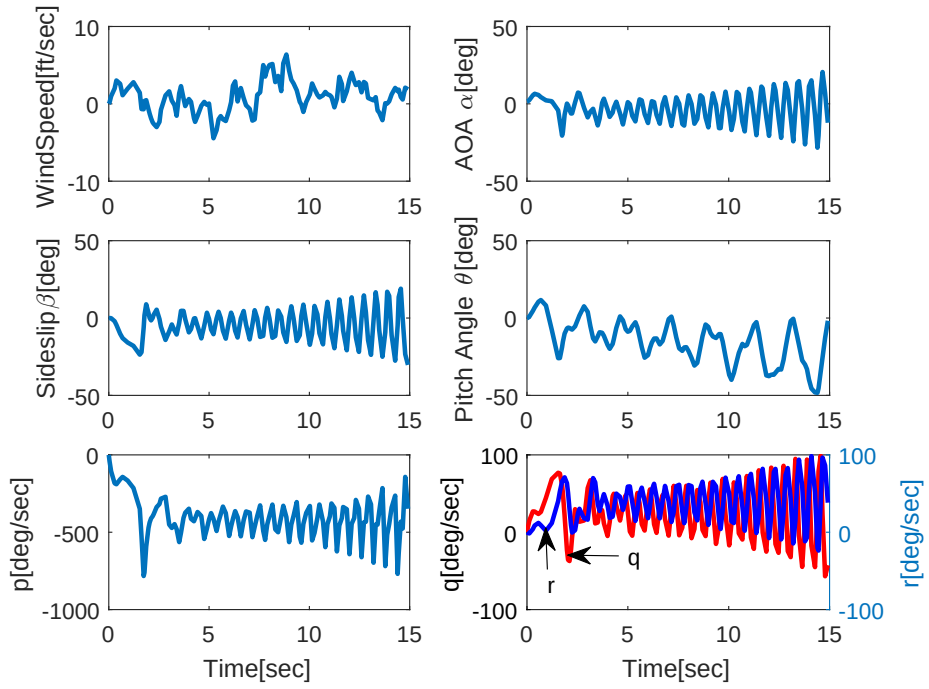

Figure 2: Open loop response of the aircraft under turbulence for $\delta_a = 25\ deg,\ \delta_e = -5\ deg$

6. Simulation Results

In this section, the performances of the designed flight controllers (FTS with DSM and FTS with STW signals) are evaluated. Simulation is performed for the swept-wing fighter model of [45, 46] for the two Flight Conditions(FC), FC 1 with ($Mach(M) = 0.9,\ H = 20,000ft$) and FC 2 with ($M = 0.7,\ H = 0ft$). The complete set of model parameters is given in [45, 46] (see appendix). It is noted that although the control surface deflection-dependent terms in $\dot{\alpha}$ and $\dot{\beta}$ were ignored for design, these terms are included in the aircraft dynamics to examine the effect of control forces on responses. Since the value of $y_{\delta r}$ is not given in [46], it is taken to be zero. Here, $\alpha_0 = 1.5$ deg and $\theta_0 = 0$. The initial state vector is $x(0) = 0$, except $\alpha(0) = 1.5$ deg.

For generating smooth command trajectories $\phi_r(t)$ and $\theta_r(t)$, or $\phi_r(t)$, and $\alpha_r(t)$, fourth-order reference generators are given by

$$(s^4 + \mu_3 s^3 + \mu_2 s^2 + \mu_1 s + \mu_0)\phi_r = \mu_0 \phi^*$$

$$(s^4 + \mu_3 s^3 + \mu_2 s^2 + \mu_1 s + \mu_0)\theta_r = \mu_0 \theta^*$$

and

$$(s^4 + \mu_3 s^3 + \mu_2 s^2 + \mu_1 s + \mu_0)\alpha_r = \mu_0 \alpha^*$$

are considered, where target values for the roll angle, the pitch angle, and the angle of attack are ϕ^*, θ^*, and α^*. The poles of the command generators are chosen to be [-3 -4 -5 -6]. The initial conditions for the command generators (except $\alpha_r(0) = 1.5$ deg) are assumed to be zero. The reference sideslip angle $\beta_r(t)$ is identically zero. The target roll angle is $\phi^* = 360$ deg and α^* is 10 or 15 (deg).

The selected feedback gains in the control input v_f are $k_{11} = k_{12} = k_{13} = 4$, $k_{21} = k_{22} = k_{23} = 4$, and the exponents $\nu_{11} = \nu_{12} = \nu_{13} = 0.25$, $\nu_{21} = \nu_{22} = \nu_{23} = 0.4$, $\epsilon_i = 0.99,\ i = 1, 2, 3$. The sliding mode controller's gain is G=diag([0.1 0.1 0.01]). Although the set of parameters exist that satisfy a sufficient condition for finite time stability, the design parameters that have been selected here are based on the observation of simulated responses. For practical reasons, limits on the control surface deflections are introduced such that $|\delta_a| \leq 30$ deg, $|\delta_r| \leq 30$ deg, and $|\delta_e| \leq 30$ deg.

In subsequent subsections, the set of actual inertia and aerodynamic parameters, and the perturbed parameters at the flight condition j are denoted as $\mathscr{P}_{FCj}$ and $\mathscr{P}_{PFCj}$, respectively. It is assumed that $\mathscr{P}_{PFCj}$=f_u*$\mathscr{P}_{FCj}$, where the uncertainty factor is $f_u = 0.7$ (i.e. -30% uncertainty). For the purpose of design, the parameters from the perturbed set $\mathscr{P}_{PFCi}$ are used, but for simulation, dynamics of the aircrafts are computed using the actual set $\mathscr{P}_{FCj}$ of parameters for the choice of $i, j = 1, 2$. For the synthesis of the control law, $\dot{\theta}$, $\dot{\alpha}$ and $\dot{\beta}$ are required. Although $\dot{\alpha}$ and $\dot{\beta}$ can be obtained using measured signals, these signals are computed by substituting the perturbed parameters of $\mathscr{P}_{PFCj}$ in $\dot{\alpha}$, and $\dot{\beta}$ given in Eq.(1). This way, it will be possible to evaluate the robustness of the control laws.

6.1. Finite Time (ϕ, θ, β) control with FTS and DSM control Laws

Now the performance of the closed-loop system, including the complete aircraft model Eq.(1) and the composite control law FTS and DSM without turbulence and under turbulence, is examined.

Case I: The aircraft was assumed to be flying at FC 1, and therefore Eq.(1) was implemented using the actual parameter set $\mathscr{P}_{FC1}$. However, the control law, $\dot{\theta}$, and $\dot{\beta}$ were computed using the perturbed parameters from the set $\mathscr{P}_{PFC2}$. Terminal values of ϕ, θ, and β were taken as $(\phi^*, \theta^*, \beta^*) = (90, 60, 0)$ deg. Selected responses are shown in figure(3).

A smooth trajectory tracking is observed. The steady-state tracking error is nearly zero at 2 sec. The maximum value of β is less than 0.08 deg. The controller saturates over a brief interval but exhibits chattering.

Case II: The aircraft was assumed to be flying in the previous condition with the same parameters, but under the turbulence of the strength applied in figure(2). The terminal values of ϕ, θ, and β are taken as $(\phi^*, \theta^*, \beta^*) = (90, 60, 0)$ deg. Selected responses are shown in figure(4).

Control input is bounded between 30 deg, but exhibits a very minimal amount of chattering in the input. A smooth trajectory tracking is observed. The steady-state tracking error is nearly zero at 2.4 sec. The maximum value of β is less than 0.05 deg. The controller saturates over a brief interval, but exhibits chattering.

6.2. Finite Time (ϕ, θ, β) control with FTS and STW control Laws

Case I: The aircraft was assumed to be flying at FC 1, and therefore Eq.(1) was implemented using the actual parameter set $\mathscr{P}_{FC1}$. However, the control law, $\dot{\alpha}$, and $\dot{\beta}$ were computed using the perturbed parameters from the set $\mathscr{P}_{PFC2}$. The terminal values of ϕ, θ, and β are taken as $(\phi^*, \theta^*, \beta^*) = (90, 60, 0)$ deg. Selected responses are shown in figure(5).

A smooth trajectory tracking is observed. The steady-state tracking error is nearly zero at 4 sec. The maximum value of β is less than 0.18 deg. The controller saturates over a brief interval and completely eliminates control input chattering, which is present in figure(3).

Case II: The aircraft was assumed to be flying in the previous condition using the very same parameters but under air turbulence of the strength applied in figure(2). The terminal values of ϕ, θ, and β are taken as $(\phi^*, \theta^*, \beta^*) = (90, 60, 0)$ deg. Selected responses are shown in figure(6).

A smooth trajectory tracking is observed. The steady-state tracking error is nearly zero at 4.2 sec. The maximum value of β is less than 0.065 deg. The controller saturates over a brief interval and completely removes the chattering present in figure(4).

6.3. Finite Time (ϕ, α, β) control with FTS and DSM Control Laws under turbulence

Now the performance of the closed-loop system, including the complete aircraft model Eq.(1) and the composite control law FTS and DSM under turbulence of the strength applied in figure(2), is examined.

The aircraft was assumed to be flying at FC 1, and therefore Eq.(1) was implemented using the actual parameter set $\mathscr{P}_{FC1}$. However, the control laws, $\dot{\alpha}$, and $\dot{\beta}$ were computed using the perturbed parameters from the set $\mathscr{P}_{PFC2}$. The terminal values of ϕ, α, and β are taken as $(\phi^*, \alpha^*, \beta^*) = (360, 10, 0)$ deg. Selected responses are shown in figure (7). A smooth trajectory tracking is observed. The steady-state tracking error is nearly zero at 2.5 sec. The maximum value of β is less than 0.005 deg. The controller saturates over a brief interval.

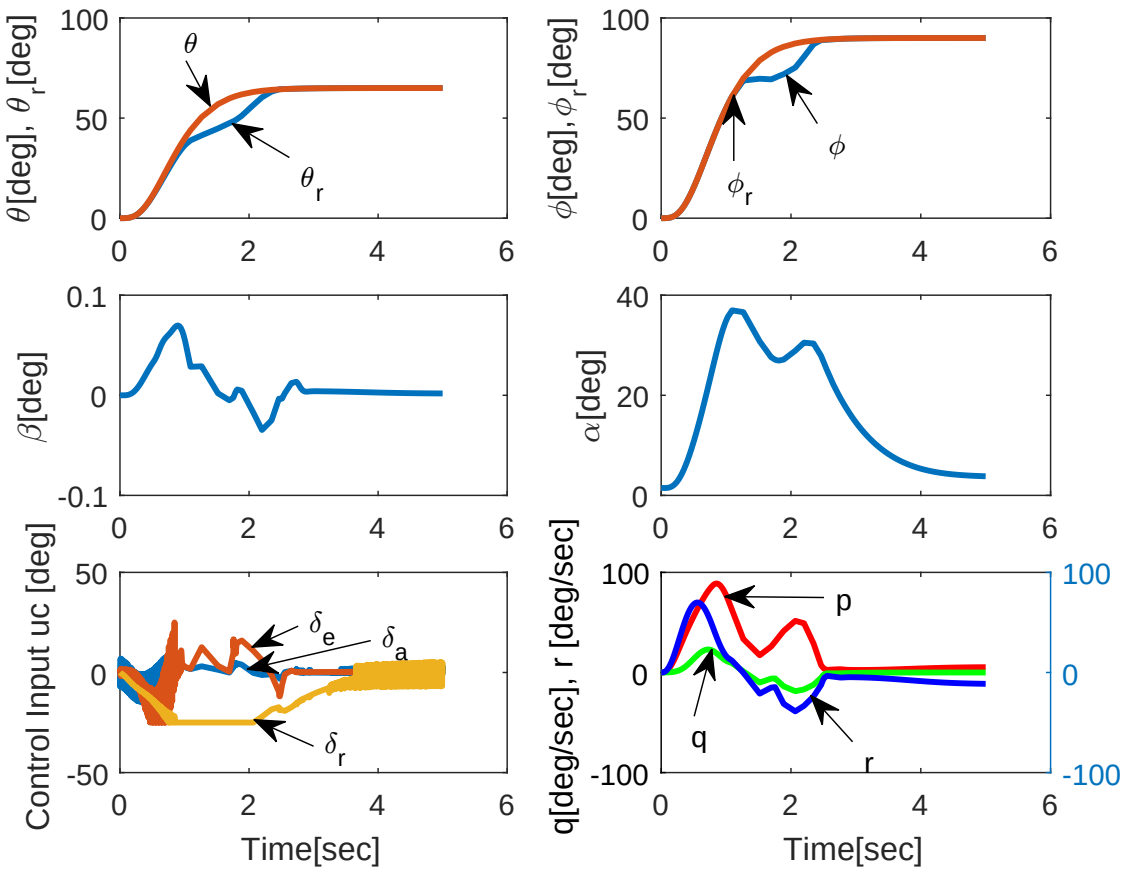
θ[deg], θr[deg]
θ
θr
φ[deg], φr[deg]
φr
φ
β[deg]
α[deg]
Control Input uc [deg]
δe
δa
δr
q[deg/sec], r [deg/sec]
p
q
r
Time[sec]
Time[sec]

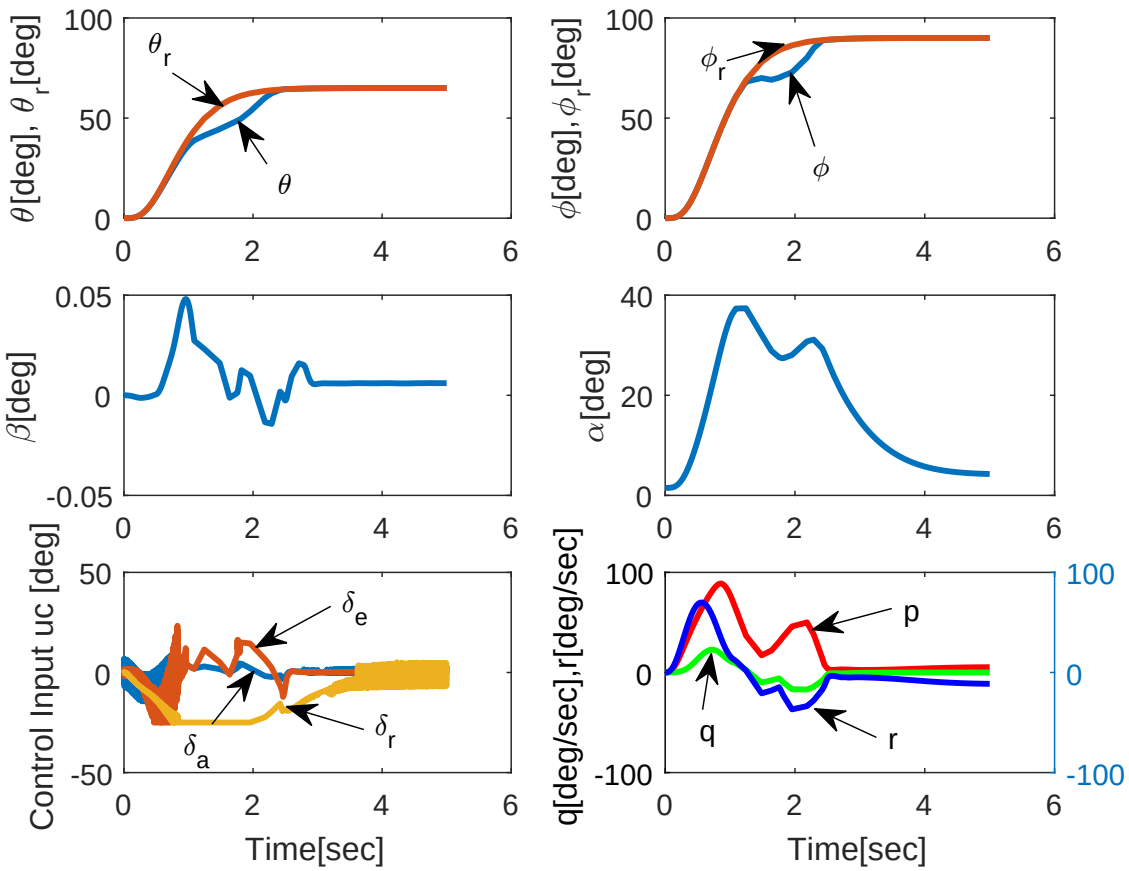
θ[deg], θ_r[deg]
θ_r
θ
100
50
0
0
2
4
6
φ[deg], φ_r[deg]
φ_r
φ
β[deg]
0.05
0
-0.05
α[deg]
40
20
Control Input uc [deg]
50
-50
δ_e
δ_a
δ_r
Time[sec]
q[deg/sec],r[deg/sec]
p
q
r
-100

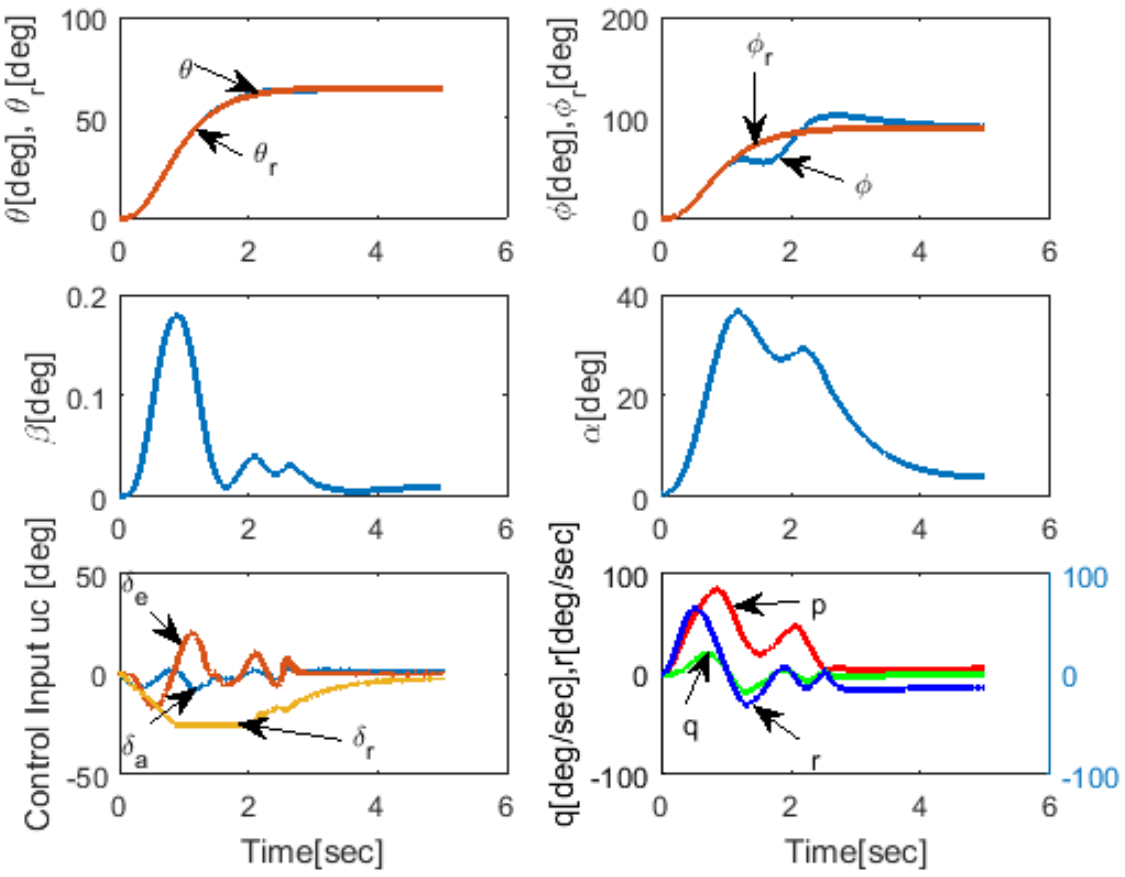
θ[deg], θr[deg]
θ
θr
ϕ[deg],ϕr[deg]
ϕr
ϕ
β[deg]
α[deg]
Control Input uc [deg]
δe
δa
δr
q[deg/sec],r[deg/sec]
p
q
r
Time[sec]
Time[sec]

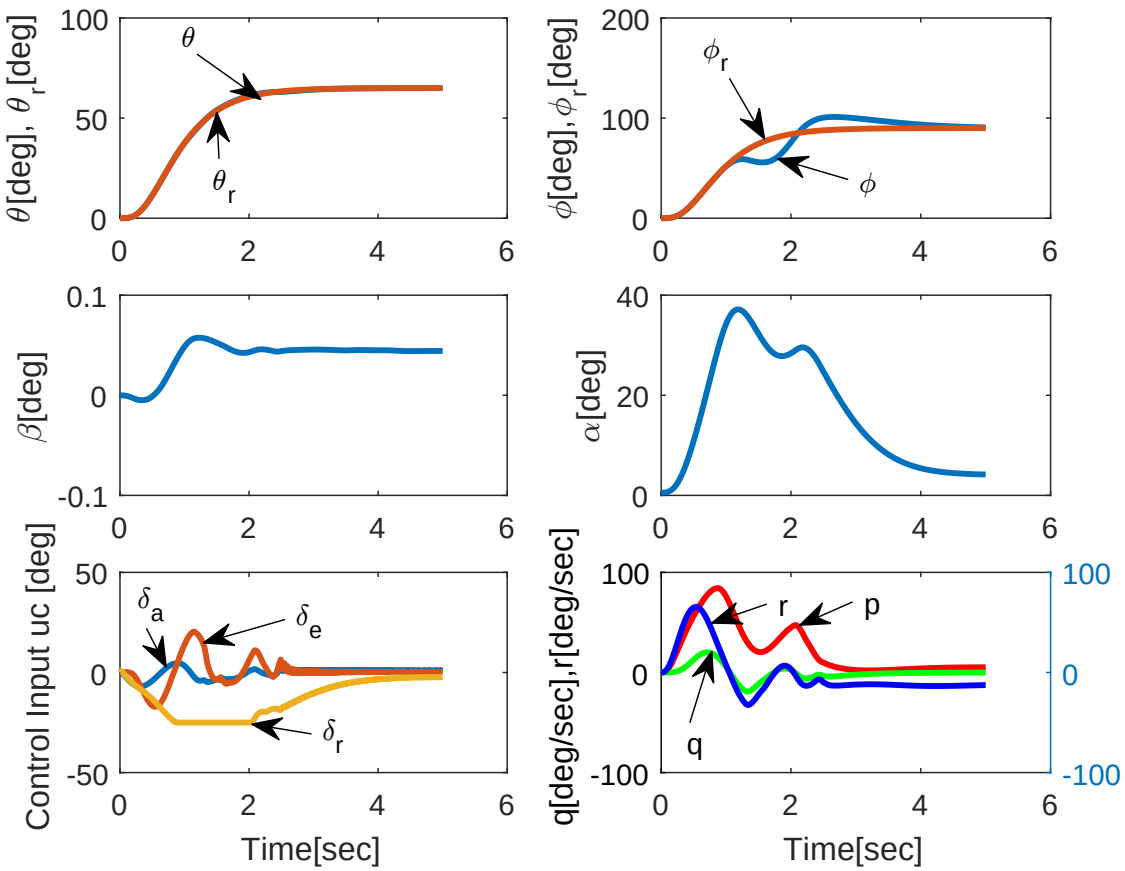
θ[deg], θr[deg]
θ
θr
100
50
0
0
2
4
6
ϕ[deg], ϕr[deg]
ϕr
ϕ
200
100
0
β[deg]
0.1
0
-0.1
α[deg]
40
20
Control Input uc [deg]
δa
δe
δr
50
-50
q[deg/sec],r[deg/sec]
r
p
q
-100
Time[sec]

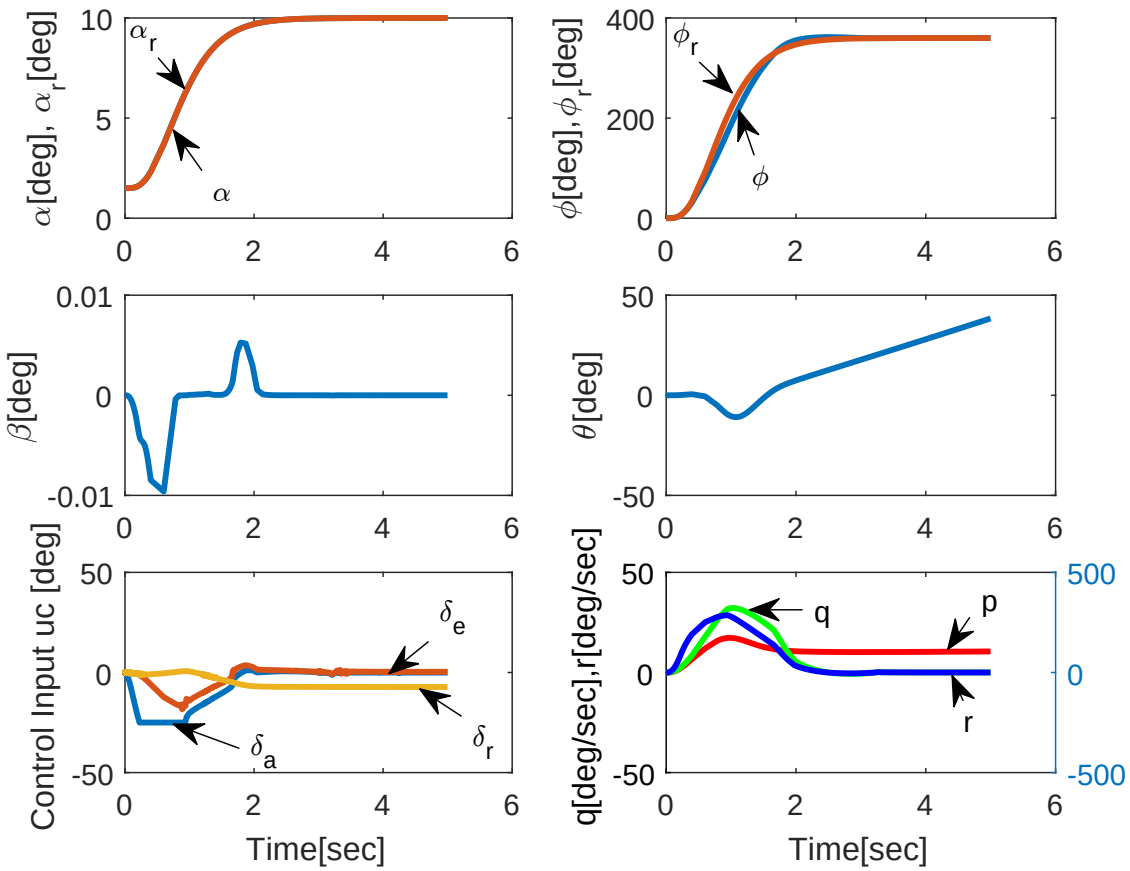
α[deg], α_r[deg]
α_r
α
φ[deg], φ_r[deg]
φ_r
φ
β[deg]
θ[deg]
Control Input uc [deg]
δ_e
δ_a
δ_r
q[deg/sec],r[deg/sec]
q
p
r
Time[sec]
Time[sec]

6.4. Finite Time (ϕ, α, β) control with FTS and STW control Laws

Now the performance of the closed-loop system including the complete aircraft model Eq.(1) and the composite control law FTS and STW is examined.

Case I: The aircraft was assumed to be flying at FC 1, at actual parameter. But the control law, $\dot{\alpha}$, and $\dot{\beta}$ were computed using the perturbed parameters from the set $\mathscr{P}_{PFC2}$. The terminal value of ϕ, α, and β is taken as $(\phi^*, \alpha^*, \beta^*) = (360, 10, 0)$ deg. Selected responses are shown in figure(8). A smooth trajectory tracking is observed. The steady-state tracking error is nearly zero at 4 sec. The maximum value of β is less than 0.1 deg. The controller saturates over a brief interval with a very small spurt of chattering.

Case II: In this case, the aircraft was assumed to be flying in the previous condition using the same parameters, but under the influence of air turbulence of the strength applied in figure(2). Selected responses are shown in figure(9).

A smooth trajectory tracking is observed. The steady-state tracking error is nearly zero at 4.2 sec. The maximum value of β is less than 0.005 deg. The controller saturates over a brief interval.

Effect of Turbulence on trajectory tracking and control inputs

The Simulation was performed using different strength of gust. The performance of the flight controller under wind turbulence is summarized in the table.

wg_max (ft/s)	Strength of turbulence wrt Fig.(2)	(ϕ, θ, β)						(ϕ, α, β)					
		FTS+DSM			FTS+STW			FTS+DSM			FTS+STW		
		CT(s)	$\beta(deg)$	$uc(deg)$	CT(s)	$\beta(deg)$	$uc(deg)$	CT(s)	$\beta(deg)$	$uc(deg)$	CT(s)	$\beta(deg)$	$uc(deg)$
3.9	0.3 X	2.42	0.043	25	4.5	0.07	25	3.3	0.08	25	3.5	0.09	25
12.15	1 X	2.42	0.047	25	4.5	0.15	25	3.3	0.33	25	4	0.4	30
24.89	2 X	2.5	0.1	25	4.5	0.3	30	1.3	0.6	35	2.5	0.9	30

Table 1: Effect of Turbulence on Aircraft control

Here, CT, wg_{max}, and uc are convergence time, maximum value of vertical wind velocity, and control input, respectively. The summary of the effect of turbulence on the aircraft control for both controllers for two sets of output variables (ϕ, θ, β and ϕ, α, β) is provided in Table 1. The effect of turbulence depicted in figure (2) for open-loop aircraft systems is taken as a reference strength of turbulence. The response of the robust DSM with turbulence depicted in figure(4) is very similar to figure(3) which is without the turbulence. Responses for robust STW with turbulence for (ϕ, θ, β) control, robust DSM with Turbulence for (α, ϕ, β) control and robust STW with turbulence for (α, ϕ, β) control are depicted in figures 6, 7, and 9, respectively. When twice the strength of turbulence is applied for trajectory tracking of the output (ϕ, α, β), a DSM control magnitude of 30 deg is found to be insufficient to stabilize the system. Hence magnitude had to be increased. A 35 deg DSM controller input is found to be sufficient enough to provide satisfactory performance and stability for the aircraft systems. As we increase the strength of the wind gust, demand for higher control input arises. Here, Input is clamped at 30 deg for practical reasons. Effect of fault coupled with turbulence was not considered for the table.

Performance under Turbulence and Partial Loss of Control Surface Effectiveness

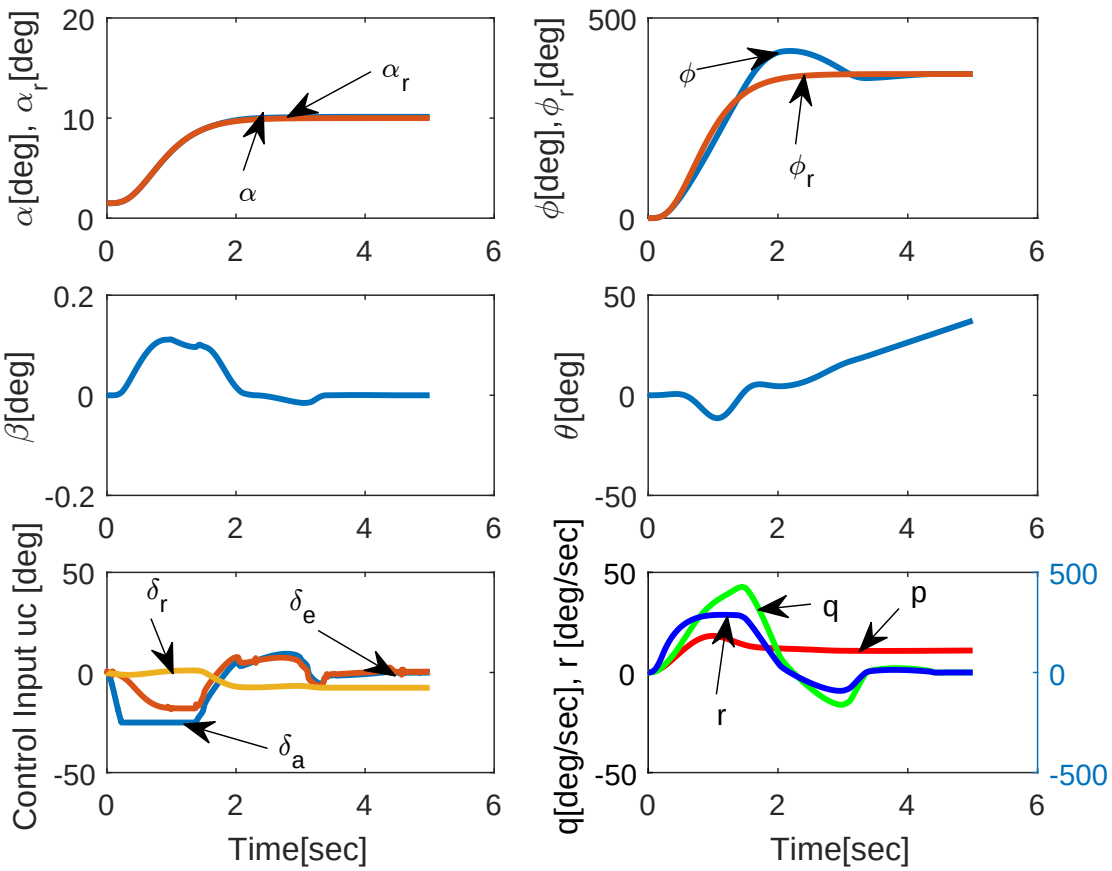
α[deg], α_r[deg]
α_r
α
φ[deg], φ_r[deg]
φ
φ_r
β[deg]
θ[deg]
Control Input uc [deg]
δ_r
δ_e
δ_a
q[deg/sec], r [deg/sec]
q
p
r
Time[sec]
Time[sec]

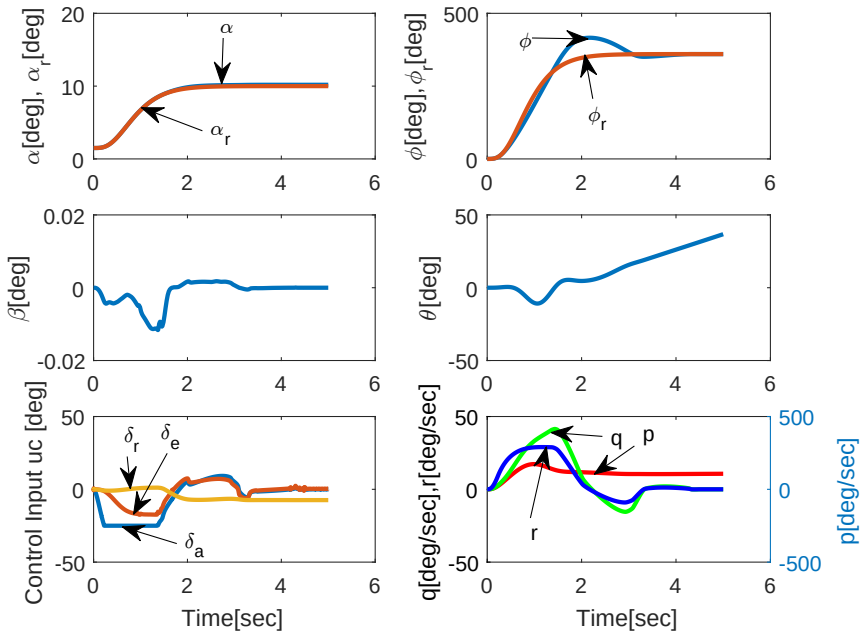

Figure 9: Robust STW with turbulence for $\alpha = 10\ deg, \phi = 360\ deg$ FC2-0.7∗FC1

Now the aircraft was assumed to be flying under the influence of air turbulence of the strength applied in figure(2), at FC 1 with a maximum value of vertical wind velocity of 12.15 ft/sec, and Eq.(1) was implemented using the actual parameter set $\mathscr{P}_{FC1}$. However, the control law, $\dot{\alpha}$, and $\dot{\beta}$ were computed using the perturbed parameters from the set $\mathscr{P}_{PFC2}$. The terminal values of ϕ, θ, and β are taken as $(\phi^*, \theta^*, \beta^*) = (90, 60, 0)$ deg. Assuming a partial degradation of control surfaces occurs at 3 seconds and remains in the perpetuity. Fault scenarios were assumed to be control surface degradation of aileron(δ_a) by 30%, rudder(δ_r) by 20%, and elevator(δ_e) by 10%. A simulation was done to examine the effect of fault when aircraft was flying under turbulence.
These responses are depicted in figure (10). As expected, there was small transient oscillation(represented by an ellipse) in the response at the time fault was introduced but thereafter tracking error converges to zero. As shown in the figure, the controller dealt with the fault scenario very efficiently. A smooth trajectory tracking is observed after a brief oscillation. The steady-state tracking error is nearly zero at 4.5 sec. The maximum value of β is around 0.35 deg, previously it was 0.065 deg without fault but under turbulence . Simulation results validate the effectiveness of the control law, which brought the faulty system back to stability, despite partial degradation of control surfaces. Simulation results for faults without turbulence have been obtained but not provided to save space.

Both controllers, DSM and STW for key output variables (ϕ, θ, β) or (ϕ, α, β), provide satisfactory results under 30 deg of input saturation. To this end, it is appropriate to compare the performance of the two controllers. DSM provides faster output tracking with a comparatively small sideslip angle than the STW controller. Continuous STW control attenuates input chattering and provides smoother input response than the DSM control. For example, small chattering in figure(3) is attenuated by the STW control in figure (5). The same pattern is followed between figures (4) and (6), (7) and (9) etc. For the chosen values of design parameters, both controllers provide robust performance. Furthermore, the structure of the DSM law is simple compared to that of the STW law, in which extra parameters p_0 and p_1 need to be tuned.

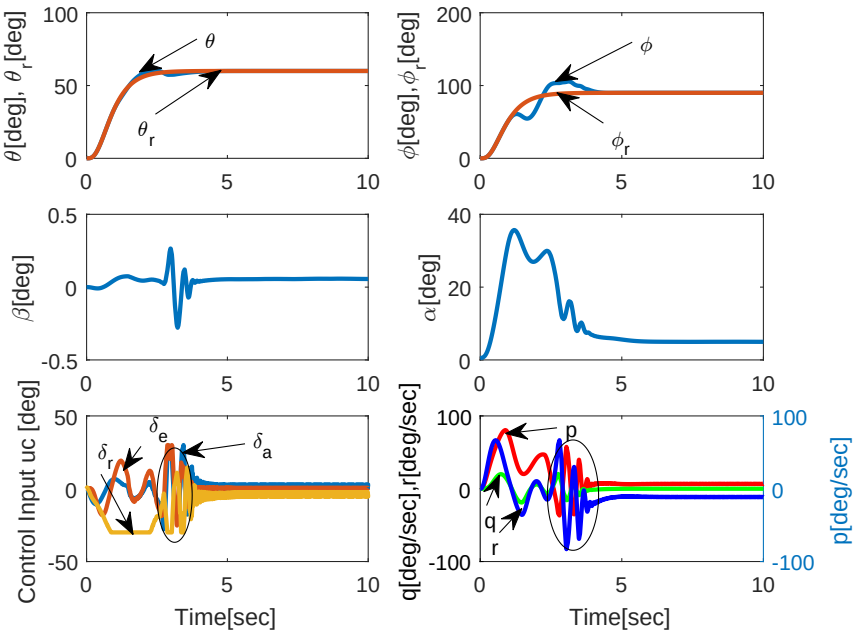

Figure 10: STW with turbulence and fault($\delta_a = 30\%, \delta_r = 20\%, \delta_e = 10\%$) at FC2-0.7∗FC1

7. Conclusions

In this article, two flight control systems for roll-coupled maneuvers of fighter aircraft have been designed. The first composite control system consisted of finite time stabilizing (FTS) control law and a discontinuous sliding mode (DSM) control law for robustification. Then, the second composite control system, which includes FTS and super twisting (STW) control signals, is derived. Unlike the first composite (discontinuous) control system, the second flight controller includes the continuous STW signal, which is capable of attenuating the effect of control chattering. In a closed-loop system, each of the composite controllers accomplished finite time trajectory control of the output variables (ϕ, θ, β) or (ϕ, α, β), despite uncertainties in the inertia and aerodynamic parameters. It was shown by digital simulation that despite use of a simplified design model and imposed practical control surface deflection limits, each of the composite controllers achieved a precise trajectory control of the output variables under the turbulence. Further, the simulated responses show that these controllers are sufficiently robust and maintain stability in the presence of turbulence and partial loss of control effectiveness due to damage in control surfaces. The advantage of the STW over the DSM yielding smoother control signals was also seen in the simulated waveforms. There are several important questions which remain unresolved in this article. A useful future research topic could be the inclusion of control and rate constraints in the design process of higher-order sliding mode and STW controllers.

Appendix: System Parameters

The Aircraft parameters and the aerodynamic coefficients for two flight conditions of the model presented in references [45, 46] are reproduced here:

	Flight Condition I	Flight Condition II		Flight Condition I	Flight Condition II
i_1	0.727	0.727	y_β	-0.196	-0.280
i_2	0.949	0.949	$y_{\delta a}$	0.0071	0.0119
i_3	0.716	0.716	$\bar{m}_\alpha$	-23.18	-10.7
l_p	-3.933	-5.786	$m_{\delta e}$	-28.37	-31.64
l_q	0.107	0.108	$m_{\dot{\alpha}}$	-0.173	-0.251
l_r	0.126	0.221	$\bar{m}_q$	-0.814	-1.168
$l_{r\alpha}$	8.390	13.160	$n_\alpha \delta a$	1.132	2.459
$l_{\beta\alpha}$	-684.40	-543.80	n_β	5.67	8.88
$l_{\alpha\delta a}$	63.5	64.6	$n_{\delta a}$	-0.921	-1.282
$l_{\delta r}$	-7.64	-10.05	$n_{\delta r}$	-6.51	-8.30
$l_{\delta a}$	-45.83	-60.27	$n_{p\alpha}$	-1.578	-1.583
l_β	-9.990	-20.910	n_p	0.002	0.013
$z_{\delta e}$	-0.168	-.224	n_q	.223	.222
z_α	-1.329	-1.746	n_r	-0.235	-0.377
g_0/V	0.0345	0.0412	–	–	–

References

[1] R. F. Stengel, Flight dynamics, Princeton University Press, 2015.

[2] B. Wigdorowitz, Application of linearization analysis to aircraft dynamics, Journal of guidance, control, and dynamics 15 (3) (1992) 746–750.

[3] J. Wang, N. Sundararajan, Extended nonlinear flight controller design for aircraft, Automatica 32 (8) (1996) 1187–1193.

[4] L. Zhang, S. Wang, H. R. Karimi, A. Jasra, Robust finite-time control of switched linear systems and application to a class of servomechanism systems, IEEE/ASME Transactions on Mechatronics 20 (5) (2015) 2476–2485.

[5] S. K. Choudhary, optimal feedback control of a twin rotor mimo system, International Journal of Modelling and Simulation 37 (1) (2017) 46–53.

[6] S. K. Choudhary, Optimal feedback control of twin rotor mimo system with a prescribed degree of stability, International Journal of Intelligent Unmanned Systems 4 (4) (2016) 226–238.

[7] A. Schy, M. Hannah, Prediction of jump phenomena in roll-coupled maneuvers of airplanes, Journal of Aircraft 14 (4) (1977) 375–382.

[8] P.-E. Aubin, Bifurcation analysis and control of a fighter aircraft, Ph.D. thesis, Massachusetts Institute of Technology (1993).

[9] J. V. Carroll, R. K. Mehra, Bifurcation analysis of nonlinear aircraft dynamics, Journal of Guidance, Control, and Dynamics 5 (5) (1982) 529–536.

[10] G. Meyer, R. Su, L. R. Hunt, Application of nonlinear transformations to automatic flight control, Automatica 20 (1) (1984) 103–107.

[11] R. A. Hess, C. Peng, Design for robust aircraft flight control, Journal of Aircraft (2017) 1–12.

[12] P. Menon, M. Badgett, R. Walker, E. Duke, Nonlinear flight test trajectory controllers for aircraft, Journal of Guidance, Control, and Dynamics 10 (1) (1987) 67–72.

[13] S. H. Lane, R. F. Stengel, Flight control design using non-linear inverse dynamics, Automatica 24 (4) (1988) 471–483.

[14] S. A. Snell, D. F. Enns, W. L. Garrard, Nonlinear inversion flight control for a supermaneuverable aircraft, Journal of guidance, control, and dynamics 15 (4) (1992) 976–984.

[15] M. Azam, S. N. Singh, Invertibility and trajectory control for nonlinear maneuvers of aircraft, Journal of Guidance, Control, and Dynamics 17 (1) (1994) 192–200.

[16] D. Bugajski, D. Enns, M. Elgersma, A dynamic inversion based control law with application to the high angle-of-attack research vehicle, in: Guidance, Navigation and Control Conference, 1990, p. 3407.

[17] D. Enns, Robustness of dynamic inversion vs mu synthesis-lateral-directional flight control example, in: Guidance, Navigation and Control Conference, 1990, p. 3338.

[18] J. Reiner, G. J. Balas, W. L. Garrard, Robust dynamic inversion for control of highly maneuverable aircraft, Journal of Guidance, control, and dynamics 18 (1) (1995) 18–24.

[19] J. Slotine, W. Li, Applied nonlinear control, prentice-hall, englewood cliffs, nj, 1991, Google Scholar.

[20] S. P. Bhat, D. S. Bernstein, Geometric homogeneity with applications to finite-time stability, Mathematics of Control, Signals and Systems 17 (2) (2005) 101–127.

[21] M. Defoort, T. Floquet, A. Kokosy, W. Perruquetti, A novel higher order sliding mode control scheme, Systems & Control Letters 58 (2) (2009) 102–108.

[22] Y. Shtessel, J. Buffington, S. Banda, Multiple timescale flight control using reconfigurable sliding modes, Journal of Guidance, Control, and Dynamics 22 (6) (1999) 873–883.

[23] I. A. Shkolnikov, Y. B. Shtessel, Aircraft nonminimum phase control in dynamic sliding manifolds, Journal of Guidance, Control, and Dynamics 24 (3) (2001) 566–572.

[24] K. W. Lee, P. R. Nambisan, S. N. Singh, Adaptive variable structure control of aircraft with an unknown high-frequency gain matrix, Journal of guidance, control, and dynamics 31 (1) (2008) 194–203.

[25] S. N. Singh, M. L. Steinberg, A. Page, Nonlinear adaptive and sliding mode flight path control of f/a-18 model, IEEE Transactions on Aerospace and Electronic Systems 39 (4) (2003) 1250–1262.

[26] S. N. Singh, M. Steinberg, Adaptive control of feedback linearizable nonlinear systems with application to flight control, Journal of Guidance, Control, and Dynamics 19 (4) (1996) 871–877.

[27] J. Farrell, M. Sharma, M. Polycarpou, Backstepping-based flight control with adaptive function approximation, Journal of Guidance, Control, and Dynamics 28 (6) (2005) 1089–1102.

[28] J. Farrell, M. Polycarpou, M. Sharma, Adaptive backstepping with magnitude, rate, and bandwidth constraints: Aircraft longitude control, in: American Control Conference, 2003. Proceedings of the 2003, Vol. 5, IEEE, 2003, pp. 3898–3904.

[29] M. Sharma, Flight-path angle control via neuro-adaptive backstepping, in: AIAA Guidance, Navigation, and Control Conference and Exhibit, 2002, p. 4451.

[30] L. Sonneveldt, Q. Chu, J. Mulder, Nonlinear flight control design using constrained adaptive backstepping, Journal of Guidance, Control, and Dynamics 30 (2) (2007) 322–336.

[31] C.-Y. Li, W.-X. Jing, C.-S. Gao, Adaptive backstepping-based flight control system using integral filters, Aerospace Science and Technology 13 (2-3) (2009) 105–113.

[32] S. Sadati, M. S. Parvar, M. Menhaj, M. Bahrami, Backstepping controller design using neural networks for a fighter aircraft, European Journal of Control 13 (5) (2007) 516–526.

[33] A. J. Calise, S. Lee, M. Sharma, Development of a reconfigurable flight control law for tailless aircraft, Journal of Guidance, Control, and Dynamics 24 (5) (2001) 896–902.

[34] D.-H. Shin, Y. Kim, Reconfigurable flight control system design using adaptive neural networks, IEEE Transactions on Control Systems Technology 12 (1) (2004) 87–100.

[35] A. J. Calise, R. T. Rysdyk, Nonlinear adaptive flight control using neural networks, IEEE control systems 18 (6) (1998) 14–25.

[36] D. Karagiannis, A. Astolfi, Non-linear and adaptive flight control of autonomous aircraft using invariant manifolds, Proceedings of the Institution of Mechanical Engineers, Part G: Journal of Aerospace Engineering 224 (4) (2010) 403–415.

[37] Y. Kobayashi, M. Takahashi, Design of nonlinear adaptive flight control system based on immersion and invariance, in: AIAA Guidance, Navigation, and Control Conference, 2009, p. 6174.

[38] K. Lee, S. Singh, Attractive manifold-based noncertainty-equivalent adaptive control of aircraft, in: 49th AIAA Aerospace Sciences Meeting including the New Horizons Forum and Aerospace Exposition, 2011, p. 80.

[39] S. Singh, M. Steinberg, A. Page, Adaptive control of high-performance aircraft with multiple control effectors, in: Guidance, Navigation, and Control Conference and Exhibit, 1999, p. 4280.

[40] R. K. Mehra, J. V. Carroll, Global stability and control analysis of aircraft at high angles-of-attack., Tech. rep., Scientific Systems INC Cambridge MA (1979).

[41] J. Young, A. Schy, K. Johnson, Pseudosteady state analysis of nonlinear aircraft maneuvers, in: 6th Atmospheric Flight Mechanics Conference, 1980, p. 1600.

[42] J. Planeaux, T. Barth, High-angle-of-attack dynamic behavior of a model high-performance fighter aircraft, in: 15th Atmospheric Flight Mechanics Conference, 1988, p. 4368.

[43] K. Raj, V. Muthukumar, S. Singh, Robust higher-order sliding mode control systems for roll-coupled maneuvers of aircraft using output feedback, in: 2018 Atmospheric Flight Mechanics Conference, 2018, p. 2833.

[44] A. Levant, A. Pridor, R. Gitizadeh, I. Yaesh, J. Z. Ben-Asher, Aircraft Pitch Control via Second-Order Sliding Technique, Journal of Guidance Control Dynamics 23 (2000) 586–594.

[45] T. Hacker, C. Oprişiu, A discussion of the roll-coupling problem, Progress in aerospace sciences 15 (1974) 151–180.

[46] D. W. Rhoads, A theoretical and experimental study of airplane dynamics in large-disturbance maneuvers, Journal of the Aeronautical Sciences 24 (7) (1957) 507–526.

[47] A. Levant, Homogeneity approach to high-order sliding mode design, Automatica 41 (5) (2005) 823–830.

[48] Y. Shtessel, C. Edwards, L. Fridman, A. Levant, Sliding mode control and observation, Vol. 10, Springer, 2014.

[49] B. K. Mukherjee, M. Sinha, Extreme aircraft maneuver under sudden lateral cg movement: Modeling and control, Aerospace Science and Technology 68 (2017) 11–25.

[50] J.-G. Sun, S.-L. Xu, S.-M. Song, X.-J. Dong, Finite-time tracking control of hypersonic vehicle with input saturation, Aerospace Science and Technology 71 (2017) 272–284.

[51] J. A. Moreno, M. Osorio, A lyapunov approach to second-order sliding mode controllers and observers, in: Decision and Control, 2008. CDC 2008. 47th IEEE Conference on, IEEE, 2008, pp. 2856–2861.

[52] J. A. Moreno, M. Osorio, Strict lyapunov functions for the super-twisting algorithm, IEEE transactions on automatic control 57 (4) (2012) 1035–1040.

[53] S. Gage, Creating a unified graphical wind turbulence model from multiple specifications, in: AIAA Modeling and simulation technologies conference and exhibit, 2003, p. 5529.

[54] K. W. Iliff, Identification and stochastic control of an aircraft flying in turbulence, Journal of Guidance, Control, and Dynamics 1 (2) (1978) 101–108.

[55] S. K. Kommuri, M. Defoort, H. R. Karimi, K. C. Veluvolu, A robust observer-based sensor fault-tolerant control for pmsm in electric vehicles, IEEE Transactions on Industrial Electronics 63 (12) (2016) 7671–7681.

[56] Y. Zhang, J. Jiang, Bibliographical review on reconfigurable fault-tolerant control systems, Annual Reviews in Control 32 (2) (2008) 229 – 252.

[57] B. Jung, Y. Kim, C. Ha, Fault tolerant flight control system design using a multiple model adaptive controller, Proceedings of the Institution of Mechanical Engineers, Part G: Journal of Aerospace Engineering 223 (1) (2009) 39–50.

[58] Y. Li, H. R. Karimi, Q. Zhang, D. Zhao, Y. Li, Fault detection for linear discrete time-varying systems subject to random sensor delay: a riccati equation approach, IEEE Transactions on Circuits and Systems I: Regular Papers 65 (5) (2018) 1707–1716.

[59] S. T. Kandukuri, A. Klausen, H. R. Karimi, K. G. Robbersmyr, A review of diagnostics and prognostics of low-speed machinery towards wind turbine farm-level health management, Renewable and Sustainable Energy Reviews 53 (2016) 697–708.